Graefes Arch Clin Exp Ophthalmol (2010) 248:1415–1422
DOI 10.1007/s00417-010-1384-z

BASIC SCIENCE

Amelioration of diabetic retinopathy by engrafted human adipose-derived mesenchymal stem cells in streptozotocin diabetic rats

Zhikun Yang · Kanghua Li · Xi Yan · Fangtian Dong · Chunhua Zhao

Received: 5 January 2010 / Revised: 18 March 2010 / Accepted: 2 April 2010 / Published online: 2 May 2010

Abstract
Background Diabetic retinopathy is a common complication of diabetes, which is caused by injury to retinal microvasculature and neurons. Mesenchymal stem cells (MSCs), which proved to have multi-linkage differentiation capacity, including endothelial cells and neurons, might be a promising cell therapy resource. The current pilot study was performed using the streptozotocin (STZ) rat model of diabetic retinopathy injected intravenously with human adipose-derived mesenchymal stem cells (AMSCs) in an effort to investigate the potency and possible therapeutic effects of AMSCs.
Methods Four experimental groups of Wistar rats were included in the current study: an untreated control group of STZ diabetic rats (n=10), a normal non-diabetic control group (n=20), an AMSC therapy group of STZ diabetic rats (n=50), and a sham group of STZ diabetic rats (n=50). Blood glucose levels were monitored closely. Immunofluorescence was used to study AMSC distribution and differentiation. The integrity of the blood-retinal barrier (BRB) was evaluated by Evans blue dye infusion to evaluate the therapeutic effects.
Results After 1 week of transplantation, a significant reduction in blood glucose levels was observed in the AMSC therapy group relative to the sham group. BRB integrity was also improved, as less Evans blue dye leakage was observed. Donor cells were observed in the retinas of therapy group rats, and they expressed rhodopsin and glial fibrillary acidic protein (GFAP), specific markers for photoreceptors and astrocytes, respectively.
Conclusions Taken together, the results of the current study suggest that AMSCs may improve the integrity of the BRB in diabetic rats by differentiation into photoreceptor and glial-like cells in the retina and by reducing the blood glucose levels. Furthermore, the data presented herein provide evidence that AMSCs may serve as a promising therapeutic approach for diabetic retinopathy.

Keywords Diabetic retinopathy (DR) · Adipose-derived mesenchymal stem cells (AMSCs) · Blood-retinal barrier (BRB)

Zhikun Yang and Kanghua Li contributed equally to this work.

Z. Yang · F. Dong (✉)
Department of Ophthalmology,
Peking Union Medical College Hospital,
No. 1 Shuaifuyuan Road Dongcheng District,
Beijing, China 100730
e-mail: d_fangtian@sina.com

K. Li · X. Yan · C. Zhao (✉)
Institute of Basic Medical Sciences and Chinese Academy of Medical Sciences, School of Basic Medicine, Peking Union Medical College, Center of Excellence in Tissue Engineering, Beijing, China
e-mail: chunhuaz@public.tpt.tj.cn

C. Zhao
Chinese Academy of Medical Science, Peking Union Medical College, Center of Excellence in Tissue Engineering, Beijing, China 100005

Introduction

Diabetic retinopathy (DR) is the most common microvascular complication of diabetes, and it remains one of the leading causes of blindness worldwide. During the first two decades of disease, nearly all patients with type 1 diabetes and over 60% of patients with type 2 diabetes develop DR. In the Wisconsin Epidemiologic Study of Diabetic Retinopathy (WESDR), 3.6% of younger-onset patients (type 1 diabetes) and 1.6% of older-onset patients (type 2 diabetes) were blind [1].

The management of DR includes glucose regulation, blood pressure and lipid control, laser coagulation, and vitrectomy. When vitrectomy is necessary, however, successful outcomes are often limited by the severity of the disease and related complications [2]. New pharmacological therapies have been developed that target the underlying biochemical mechanisms responsible for DR-associated protein kinase C (PKC) activation, oxidative stress, angiogenesis, and the glycation and sorbitol pathway [3–5]. However, most of the previously described therapies destroy neovasculature or prevent neovascularization, but fail to eliminate pathogenic factors.

It is well known that DR is not only a microvascular disease but also a neurodegenerative disease [6]. The diabetes-associated pathological changes made to glial cells and retinal neurons occur earlier than the effects on endothelial cells. It is possible that an early injury to vascular endothelial cells could affect neuronal, microglial, or macroglial cells and their normal interactions. Alternatively, it is plausible that a metabolic insult may target neural cell function, which could in turn impair blood-retinal barrier (BRB) integrity [7].

During recent years, many studies have shown that mesenchymal stem cells (MSCs) possess extensive differentiating potentials, may contribute to the repair of different organs and tissues, and may also provide an option to retinal injury and diseases repairing. Bone marrow-derived mesenchymal stem cells (BMSCs) have been well studied in the context of retinal diseases. In contrast to BM-MSC, MSC isolated from waste human adipose tissue is easily accessed, cause less tissue damage, and therefore may be a more convenient, safer source. Furthermore, human adipose-derived mesenchymal stem cells (AMSCs) have been reported to differentiate into endothelial cells and neurons in vivo [8, 9], and our lab has demonstrated that AMSCs can differentiate into endothelial cells, photoreceptor cells, and astrocytes in a rat model of retinitis pigmentosa (RP) (our unpublished results). In order to determine whether AMSCs could be used to ameliorate the integrity of the BRB in a diabetic model, in this study, we worked on the differentiation of AMSCs in the retina of streptozotocin (STZ) induced type 1 diabetic rats, and investigated the effects of transplanted AMSCs on BRB integrity.

Materials and methods

Isolation and cultivation of human adipose-derived mesenchymal stem cells

Human adipose tissue was obtained from patients undergoing tumescent liposuction according to procedures approved by the Ethics Committee of the Chinese Academy of Medical Sciences and Peking Union Medical College. The adipose tissue was washed with HBSS (approximately 3 ml/g), resuspended in 0.075% type IA collagenase (Sigma)/HBSS (approximately 2 ml/g), and incubated at 37°C for 1 h. The digested adipose tissue was passed through a 100-μm filter to remove debris and centrifuged at 160 × *g* for 10 min to obtain a cell pellet. The pellet was resuspended and washed twice with HBSS.

After isolation, 30 ml of resuspended cells were plated in expansion medium at a density of 5×10^6 nucleated cells/100 mm tissue culture dish and incubated at 37°C in a humidified environment containing 5% CO_2. The expansion medium contained 58% DF-12 medium (Dulbecco's modified Eagle's medium/Ham's F-12 medium, Gibco), 40% MCDB (medium complete with trace elements-201, Sigma), 2% FCS (Gibco), 1× insulin-transferrin-selenium (ITS, Gibco), 1×10^{-9}mol/l dexamethasone (Sigma), 1×10^{-4}mol/l ascorbic acid 2-phosphate (Sigma), 20 ng/ml interleukin-6, 10 ng/ml EGF, 10 ng/ml PDGF-BB (Sigma), 100 U/ml penicillin, and 100 μg/ml streptomycin (Gibco). The third passage of human adipose-derived MSCs (AMSCs) was used for intravenous injections. The AMSCs were immunopositive for CD29, CD44, CD105, Flk-1, and immunonegative for CD31, CD34, CD45, and HLA-DR, as described previously [8].

Animals and transplantation

Principles of laboratory animal care were followed according to the OPRR Public Health Service Policy on the Humane Care and Use of Laboratory Animals and the U.S. Animal Welfare Act, as amended. Male Wistar rats weighing between 180 and 200 g were subjected to fasting conditions for a 24-h period, and were then rendered diabetic with a single intraperitoneal injection of STZ (60 mg/kg, Sigma) freshly dissolved in citrate buffer (pH 4.5). Diabetes development (as defined by blood glucose levels greater than 250 mg/dl) was verified 1 week after the STZ injection. Rats were housed in the PUMCH animal facility with a 12-h light/dark cycle and allowed free access to food and water. Fasting blood glucose levels were tested using a blood glucose meter (Roche) at 1, 2, 3, and 4 weeks after AMSC transplantation.

At 12 weeks after STZ injection, qualified diabetic rats were selected and randomly divided into two groups: a therapy group (n=50) and a sham group (n=50), which were injected intravenously through the caudal vein with 0.5 ml AMSCs (1×10^7 cells/ml) and 0.5 ml HBSS, respectively, using a 1 ml syringe. Control groups included untreated STZ diabetic rats (n=10) and normal non-diabetic rats (n=20). Five rats in the latter group were also treated with AMSCs following the same procedure, to show the

difference of AMSC distribution between the diabetic and normal organs.

Immunohistochemical studies

Five rats from each group were killed at the following time points: immediately following the transplantation (as baseline), and at 1, 2, 3, and 4 weeks post-transplantation. Both eyes were enucleated for histological and immunohistochemical examination. After transcardial perfusion with 4% paraformaldehyde in 0.1 M phosphate buffer, the eyes were embedded in paraffin and 5-μm serial sections were prepared. The specimens were deparaffinized in xylene, dehydrated in graded alcohols, rinsed with phosphate-buffered saline (PBS, pH 7.4), and incubated with 10 mM citrate buffer (pH 6.0) at 110°C for four consecutive 5-min incubations, which were supplemented with water between incubations. After washing with PBS, the specimens were blocked for 1 h at room temperature in PBS containing 1% bovine serum albumin (BSA), 0.1% Triton X-100, and 3% normal goat serum (NGS). Subsequently, sections were incubated for 1 h at room temperature with mouse anti-human nuclei antibody (1:25, Chemicon), followed by FITC-conjugated goat anti-mouse antibody (1:100, Invitrogen). After washing with PBS, the sections were incubated with mouse anti-rhodopsin antibody (1:100, Chemicon) or mouse anti-glial fibrillary acidic protein (GFAP) antibody (1:100, AbCam) for 1 h at room temperature, followed by a 30-min incubation with rhodamine-conjugated goat anti-mouse antibody. Finally, after washing with PBS, the sections were counterstained with Hoechst 33342 (Sigma) for 1 min [10].

BRB breakdown study

1. Preparation of standard curve of Evans blue dye in formamide

Evans blue dye (Sigma) was dissolved in normal saline (30 mg/ml), sonicated for 5 min in an ultrasonic cleaner, and filtered through a 5-μm filter (Millipore). Diabetic rats were anesthetized with phenobarbital (Sigma, 30 mg/kg), and additional anesthesia was provided throughout the procedures as needed. The right jugular vein and left carotid artery were cannulated with 0.28-and 0.58-mm internal diameter polyethylene tubing (Becton Dickinson), respectively, and filled with heparinized saline (400 units heparin/ml saline). The dissolved Evans blue dye was injected through the jugular vein over 10 s at a dosage of 60 mg/kg. Immediately after the Evans blue dye infusion, the rats turned visibly blue, confirming their uptake and distribution of the dye. Two minutes after the injection, 0.2 ml of blood was drawn from the carotid artery to obtain the initial plasma concentration of Evans blue dye plasma. At subsequent 20-min intervals, 0.1 ml blood was drawn from the carotid artery up to 2 h after the Evans blue dye injection to obtain the time-averaged Evans blue dye plasma concentrations. At exactly 2 h post-infusion, 0.2 ml blood was drawn from the left ventricle to obtain the final Evans blue dye plasma concentration. The blood samples were centrifuged at 16,000 × g for 15 min and diluted to 1:1,000 of their initial concentration in formamide. The absorbance was then measured with an ELISA/EIA clinical photometer (Biotech, USA) at 620 nm, which is the absorption maximum for Evans blue dye in

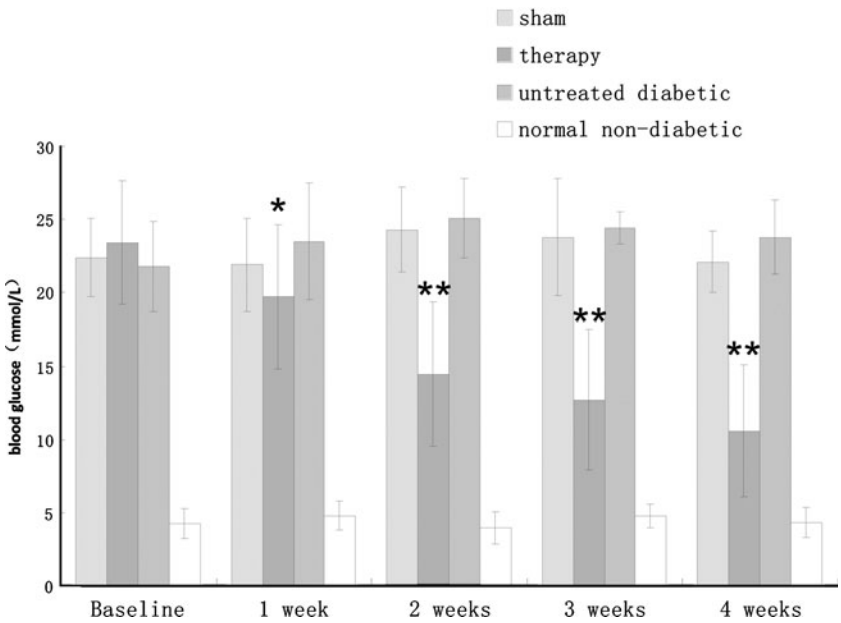

Fig. 1 Blood glucose levels in rats from the therapy, sham, and untreated diabetic control groups. Blood glucose levels decreased over time only in the therapy group (*Significantly greater than control, $p<0.05$. **Highly significantly greater than control, $p<0.01$.). There was no significant difference between the sham group and untreated diabetic control groups during the 4 weeks ($p>0.05$)

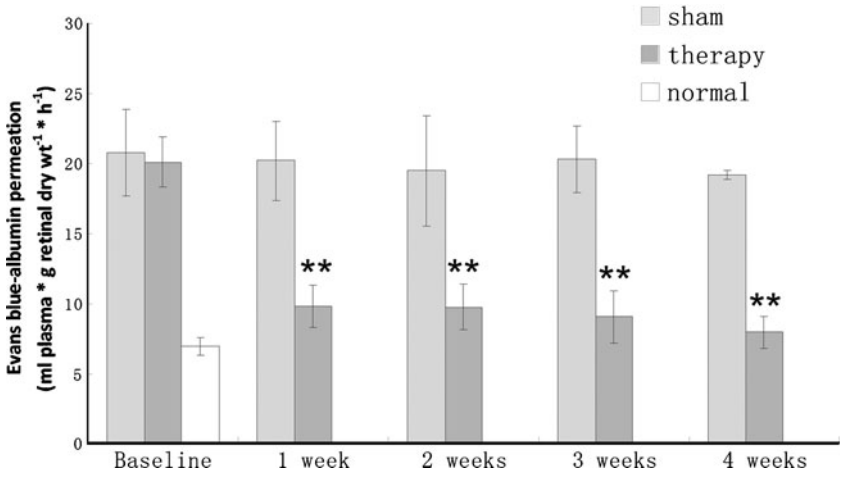

Fig. 2 BRB values in therapy, sham, and normal non-diabetic rat groups. There was a statistically significant difference between the normal non-diabetic control group and the therapy/sham group at baseline. The integrity of the BRB improved in the therapy group beginning in the first week and continuing through the fourth week (*significantly greater than control, $p<0.05$. **Highly significantly greater than control, $p<0.01$)

formamide. The concentration of the dye in the plasma was calculated based on a standard curve of Evans blue dye in formamide. Results are expressed as micrograms of Evans blue dye per microliter of plasma [11].

2. Measurement of BRB breakdown in diabetic rats with or without AMSC therapy

At 12 weeks after STZ-induced diabetes, AMSCs were injected into the rats from both the therapy group and the sham group. Five rats from the untreated non-diabetic control group (fed in the same manner as the STZ rats) were also enrolled as baseline. At each time point of 1, 2, 3, and 4 weeks post-transfusion, five rats from each group were evaluated for BRB breakdown. After the rats were anesthetized with generalized anesthesia, Evans blue dye (60 mg/kg) was injected and initial, time-averaged, and final (t=120 min blood samples were collected using the procedures outlined above. After the dye had circulated for 2 h, the chest cavity was opened and the rats were perfused via the left ventricle with citrate-buffered paraformaldehyde (1% wt/vol, pH 3.5, 37°C, Sigma). The perfusion lasted 2 min at a physiological pressure of 120 mmHg (the height of the apparatus was adjusted to allow an approximate flow rate of 66 ml/min before the catheter was inserted and perfusion initiated). A pH of 3.5 was used to optimize Evans blue dye binding to albumin, and the perfusion solution was warmed to 37°C to prevent vasoconstriction. Immediately after perfusion, both eyes were enucleated and bisected at the equator. The retinas were then carefully dissected under an operating microscope. After measuring the retinal dry weight, the Evans blue dye was extracted by incubating each retina in 0.3 ml formamide for 18 h at 70°C. The extract was ultracentrifuged (Eppendorf, Germany) at a speed of 500,000 × g for 45 min at 4°C to precipitate any proteins. Sixty microliters of the supernatant was used to determine the absorbance at 620 nm. The concentration of Evans blue dye in the extracts was calculated based on a standard curve of Evans blue dye in formamide. BRB breakdown was calculated using the following equation, and the results are expressed as μl plasma × g retinal dry wt^{-1}·h^{-1}:

3. Preparation of Evans blue dye standard curve

Evans blue dye standards dissolved in formamide maintained a reliable linear relationship between background-subtracted absorbances (620–720 nm) at concentrations ranging from 10^{-4} to 10^{-2}mg/ml (r=0.998) Standards run on different days (circles versus triangles) were virtually identical (r=0.997).

Statistical analyses

Data and statistical analyses were performed using SPSS 14.0 software. Data are presented as mean ± SD. Pairwise comparisons between groups were made using independent nonparametric tests. For all statistical tests, $p<0.05$ was considered statistically significant.

Fig. 3 AMSC distribution and differentiation in the retina. **a**–**c** HuNu staining at 1 week post-transplantation. **a** Therapy group: a large number of labeled AMSCs could be identified in the ONL, and fewer labeled AMSC cells were found in the INL and GCL. **b** Sham group: no AMSCs could be found in the retina. **c** Normal non-diabetic rats injected with AMSCs: only a small number of AMSCs could be identified in the ONL. **d**–**f** Therapy group with HuNu, Hoechst, and rhodopsin staining at 1 week post-transplantation. AMSCs were positive for HuNu and rhodopsin, indicating differentiation to rod cells (inset, higher magnification view). **g**–**i** Therapy group with HuNu, Hoechst, and GFAP staining at 1 week post-transplantation. AMSCs were positive for HuNu and GFAP, indicating differentiation to astrocytes (*arrow*). **j**–**l** Therapy group with HuNu staining at 1, 2, and 4 weeks post-transplantation. At later time points, the number of AMSCs in the ONL decreased, while the differentiated AMSCs appeared to show a more organized arrangement. *Scale bar* 50 μm ▶

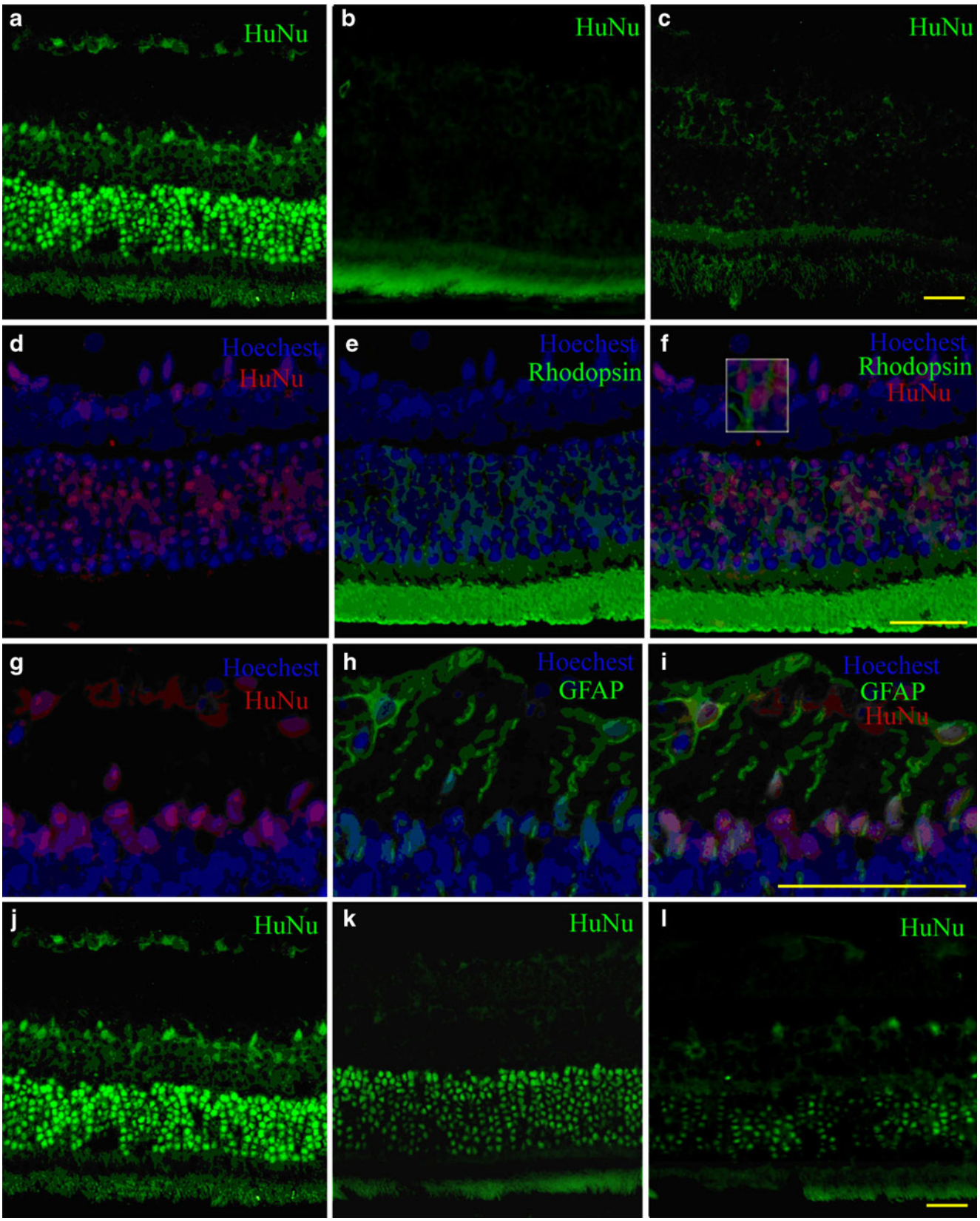
a
HuNu
b
HuNu
c
HuNu
d
Hoechest
HuNu
e
Hoechest
Rhodopsin
f
Hoechest
Rhodopsin
HuNu
g
Hoechest
HuNu
h
Hoechest
GFAP
i
Hoechest
GFAP
HuNu
j
HuNu
k
HuNu
l
HuNu

Results

Induction of diabetes

To induce diabetes in Wistar rats, intraperitoneal STZ (60 mg/kg) was administered. Most rats developed cataracts after 12 weeks, and the retina could not be examined.

Evaluation of transplantation effects

Blood glucose levels

Blood glucose levels were tested every week after transplantation. Both the untreated diabetic control group and the sham group maintained blood glucose levels between 20 and 25 mmol/l throughout the entire 4 weeks after transplantation. In contrast, the blood glucose levels in the therapy group decreased over time, and significant differences were apparent between the therapy group and untreated diabetic control/sham groups (Fig. 1, $p<0.05$, $p<0.01$, $p<0.01$, $p<0.01$, at 1, 2, 3, and 4 weeks, respectively). At 4 weeks, the blood glucose levels of the therapy group were 55% lower than baseline; however, they remained higher than the levels of non-diabetic rats.

BRB breakdown

At 12 weeks after diabetes induction, AMSCs were injected intravenously to determine whether they could protect the BRB [11]. When the BRB is impaired, more Evans blue dye leaks out from the vasculature and remains in the retina. Therefore, by comparing the concentration of Evans blue dye in retinas from different groups with or without therapy, BRB integrity could be evaluated quantitatively.

At baseline, the BRB breakdown values in the two diabetic rat groups (therapy group and sham group) were 20.8±3.1 and 20.1±1.8 ml plasma×g retinal dry $wt^{-1} \cdot h^{-1}$, respectively, which were significantly higher than that of non-diabetic rats (7.0±0.6 ml plasma×g retinal dry $wt^{-1} \cdot h^{-1}$, $p<0.01$). Beginning at 1 week post-transplantation, BRB breakdown values were significantly lower in the therapy group relative to the sham group, and this difference was maintained over the course of 4 weeks (Fig. 2). At 4 weeks, BRB breakdown was nearly completely repaired in the therapy group when compared to the normal non-diabetic control group at baseline ($p>0.05$).

Distribution and differentiation of AMSC donor cells in the retina

Retinal sections were examined to study the homing and potency of donor AMSCs. At 1, 2, 3, and 4 weeks post-transplantation, the animals were killed and the eyes were enucleated. Human AMSCs could be easily identified in the retina based on positive staining with the anti-human nuclei antibody (HuNu) (Fig. 3a), which demonstrated that the intravenously administered stem cells could be targeted to the impaired retinas. One week after transplantation, a high number of AMSCs were identified in the outer nuclear layer (ONL), and relatively fewer AMSCs were found in the inner nuclear layer (INL) and ganglion cells layer (GCL) (Fig. 3a). The retinal sections were then assayed using double immunofluorescence staining for Rhodopsin and GFAP to identify donor photoreceptor cells and astrocytes. As shown in Fig. 3d-i, donor AMSCs were capable of differentiating into both types of cells. Similar observations were made during subsequent weeks, although the number of AMSCs decreased and their arrangement became more organized (Fig. 3j-l).

Discussion

DR involves the formation of microvascular lesions and neural degeneration. Impairment of the BRB contributes to the decrease in visual acuity during the early phase of DR and during disease progression. In this study, we found that transfusion of human AMSCs led to a decrease in blood glucose levels in the STZ rat model, meanwhile engrafted AMSCs homed to retina and differentiated into photoreceptor-like cells and astrocytes-like cells induced by DR, and ameliorated the integrity of the BRB.

Embryonic stem cells (ESCs) and somatic stem cells (SSCs) had been studied widely, however, ethical issues associated with ESCs have limited their use. Recently, however, the FDA approved research using human ESCs for patients with spinal injuries. SSC research has focused primarily on the use of mesenchymal stem cells (MSCs). MSCs, which are multipotent, low immunogenic cells, and are easily obtainable from multiple tissues, have several advantages over ESCs [12, 13]. Scientists have applied MSCs in studies of retinal diseases. For example, previous studies demonstrated that MSCs could differentiate to retinal cells and endothelial cells and rescue the photoreceptors in the diseased retina [14–16]. However, the harvesting procedure required to isolate BMSCs has limited their clinical application to some extent. Relative to BMSCs, AMSCs have the following advantages: (1) the cells can be acquired by liposuction, which is more simple, safe, and comfortable for the donors; (2) large numbers of stem cells can be easily obtained without much culture and enrichment, and the risk of contamination is lower; and (3) they can differentiate into endothelial cells and neural cells with nestin expression. In the current study, we used intravenous injection of AMSCs as a stem cell therapy for DR in STZ diabetic rats [8, 17, 18].

In this study, intravenous administration of AMSCs was chosen as the delivery method due to the risk of possible endophthalmitis, retinal detachment, and hemorrhage associated with repeated intravitreous injections. The inner limiting membrane may also limit the distribution of stem cells in the retina. Furthermore, based on the fact that diabetes is a systemic disease, we hypothesized that intravenous administration of AMSCs would be more beneficial overall.

We found that blood glucose levels decreased in STZ rats when AMSCs were injected intravenously, which is consistent with the findings of Ezquer et al. [19]. Previous studies have also demonstrated the capacity of transplanted BMSCs to initiate endogenous pancreatic tissue regeneration and to inhibit damage to regenerated islet cells [20–22]. A previous study demonstrated that induced AMSCs expressed insulin, glucagon, and somatostatin [23], suggesting that they may participate in the repair of damaged pancreatic tissue and lower blood glucose levels. In this study, engrafted AMSCs differentiated to form astrocytes and photoreceptor-like cells in the STZ rat model of DR, suggesting that AMSCs may target retinal lesions and differentiate into retinal cells. We did not detect any sign of AMSC differentiation into endothelial, while our lab has demonstrated that AMSCs were capable of differentiating into endothelial, photoreceptor, and retinal pigment epithelial (RPE) cells in a rat model of RP (unpublished). It is possible that endothelial differentiation could be detected more easily using a flat-mount retina preparation; high blood glucose levels might also affect the distribution and differentiation of AMSCs.

The BRB is composed of retinal vasculature and RPE cells. The inner barrier includes endothelial cells, the basement membrane, and astrocytes, which play an important role in DR. In the current study, BRB breakdown was examined at 12 weeks after diabetes induction in STZ rats, and BRB integrity improvement was found following AMSC transplantation, although no donor-derived endothelial cells were identified. There may be several reasons for the lack of endothelial cells. Blood glucose is an important factor in maintaining the intact BRB, and decreased blood glucose levels might facilitate BRB breakdown [24]. Retinal capillaries are surrounded by the astrocytes in the retina, and Müller cells also play an important role in adjusting retinal blood flow and angiogenesis. With their potential to differentiate into astrocytes, AMSCs might provide improved support to capillaries' integrity and reduce capillary leakage [25]. Notably, studies of neurodegenerative disease have shown that some stem cells have neurotrophic effects on the retina [26]. Based on the observation that neural degeneration, which may occur earlier than changes to microvascular [6], is an important component of DR pathogenesis, it is possible that AMSCs could play a similar role in diabetic animals. In order to test this hypothesis, future studies should focus on systemic and ocular changes in neurotrophic factors [4]. VEGF is a potent cytokine that enhances vascular permeability, stimulates endothelial cell proliferation and migration, and promotes angiogenesis [27]. The levels of VEGF and its receptors, which play a key role in the development of pattern dystrophy of the retina (PDR) and macular edema, are elevated in DR. Future studies should focus on the influence of stem cells on VEGF, PEDF, and other cytokines in DR. Additionally, follow-up studies that include a control group of rats with controlled blood glucose levels could help determine whether AMSC-mediated effects on BRB integrity and blood glucose levels are separable. By focusing on expressed cytokines, it may be possible to gain insight into the molecular mechanisms underlying AMSC function.

In summary, this study found that AMSCs homed to the injured retina in STZ model and differentiated into photoreceptors and astrocytes, and demonstrated the ability of AMSCs to repair BRB breakdown in DR and to lower blood glucose levels. Accordingly, administration of AMSCs may become an effective part of the therapy for DR patient.

References

1. Fong DS, Aiello L, Gardner TW, King GL, Blankenship G, Cavallerano JD, Ferris FL 3rd, Klein R (2004) Retinopathy in diabetes. Diab Care 27(Suppl 1):S84–S87
2. Mason JO 3rd, Colagross CT, Haleman T, Fuller JJ, White MF, Feist RM, Emond TL, McGwin G Jr (2005) Visual outcome and risk factors for light perception and no light perception vision after vitrectomy for diabetic retinopathy. Am J Ophthalmol 140:231–235
3. Strom C, Sander B, Klemp K, Aiello LP, Lund-Andersen H, Larsen M (2005) Effect of ruboxistaurin on blood-retinal barrier permeability in relation to severity of leakage in diabetic macular edema. Invest Ophthalmol Vis Sci 46:3855–3858
4. Kunisaki M, Bursell SE, Clermont AC, Ishii H, Ballas LM, Jirousek MR, Umeda F, Nawata H, King GL (1995) Vitamin E prevents diabetes-induced abnormal retinal blood flow via the diacylglycerol-protein kinase C pathway. Am J Physiol 269: E239–E246
5. Freedman BI, Wuerth JP, Cartwright K, Bain RP, Dippe S, Hershon K, Mooradian AD, Spinowitz BS (1999) Design and baseline characteristics for the aminoguanidine clinical trial in overt type 2 diabetic nephropathy (ACTION II). Control Clin Trials 20:493–510
6. Barber AJ (2003) A new view of diabetic retinopathy: a neurodegenerative disease of the eye. Prog Neuropsychopharmacol Biol Psychiatry 27:283–290
7. Gardner TW, Antonetti DA, Barber AJ, LaNoue KF, Levison SW (2002) Diabetic retinopathy: more than meets the eye. Surv Ophthalmol 47(Suppl 2):S253–S262
8. Cao Y, Sun Z, Liao L, Meng Y, Han Q, Zhao RC (2005) Human adipose tissue-derived stem cells differentiate into endothelial cells in vitro and improve postnatal neovascularization in vivo. Biochem Biophys Res Commun 332:370–379

9. Safford KM, Hicok KC, Safford SD, Halvorsen YD, Wilkison WO, Gimble JM, Rice HE (2002) Neurogenic differentiation of murine and human adipose-derived stromal cells. Biochem Biophys Res Commun 294:371–379
10. Meyer JS, Katz ML, Maruniak JA, Kirk MD (2006) Embryonic stem cell-derived neural progenitors incorporate into degenerating retina and enhance survival of host photoreceptors. Stem Cells 24:274–283
11. Xu Q, Qaum T, Adamis AP (2001) Sensitive blood-retinal barrier breakdown quantitation using Evans blue. Invest Ophthalmol Vis Sci 42:789–794
12. Pittenger MF, Mackay AM, Beck SC, Jaiswal RK, Douglas R, Mosca JD, Moorman MA, Simonetti DW, Craig S, Marshak DR (1999) Multilineage potential of adult human mesenchymal stem cells. Science 284:143–147
13. Jiang Y, Jahagirdar BN, Reinhardt RL, Schwartz RE, Keene CD, Ortiz-Gonzalez XR, Reyes M, Lenvik T, Lund T, Blackstad M, Du J, Aldrich S, Lisberg A, Low WC, Largaespada DA, Verfaillie CM (2002) Pluripotency of mesenchymal stem cells derived from adult marrow. Nature 418:41–49
14. Ritter MR, Banin E, Moreno SK, Aguilar E, Dorrell MI, Friedlander M (2006) Myeloid progenitors differentiate into microglia and promote vascular repair in a model of ischemic retinopathy. J Clin Invest 116:3266–3276
15. Tomita M, Adachi Y, Yamada H, Takahashi K, Kiuchi K, Oyaizu H, Ikebukuro K, Kaneda H, Matsumura M, Ikehara S (2002) Bone marrow-derived stem cells can differentiate into retinal cells in injured rat retina. Stem Cells 20:279–283
16. Otani A, Kinder K, Ewalt K, Otero FJ, Schimmel P, Friedlander M (2002) Bone marrow-derived stem cells target retinal astrocytes and can promote or inhibit retinal angiogenesis. Nat Med 8:1004–1010
17. Di Rocco G, Iachininoto MG, Tritarelli A, Straino S, Zacheo A, Germani A, Crea F, Capogrossi MC (2006) Myogenic potential of adipose-tissue-derived cells. J Cell Sci 119:2945–2952
18. Liu Y, Yan X, Sun Z, Chen B, Han Q, Li J, Zhao RC (2007) Flk-1+ adipose-derived mesenchymal stem cells differentiate into skeletal muscle satellite cells and ameliorate muscular dystrophy in mdx mice. Stem Cells Dev 16:695–706
19. Ezquer FE, Ezquer ME, Parrau DB, Carpio D, Yanez AJ, Conget PA (2008) Systemic administration of multipotent mesenchymal stromal cells reverts hyperglycemia and prevents nephropathy in type 1 diabetic mice. Biol Blood Marrow Transplant 14:631–640
20. Wu XH, Liu CP, Xu KF, Mao XD, Zhu J, Jiang JJ, Cui D, Zhang M, Xu Y, Liu C (2007) Reversal of hyperglycemia in diabetic rats by portal vein transplantation of islet-like cells generated from bone marrow mesenchymal stem cells. World J Gastroenterol 13:3342–3349
21. Lee RH, Seo MJ, Reger RL, Spees JL, Pulin AA, Olson SD, Prockop DJ (2006) Multipotent stromal cells from human marrow home to and promote repair of pancreatic islets and renal glomeruli in diabetic NOD/scid mice. Proc Natl Acad Sci U S A 103:17438–17443
22. Hess D, Li L, Martin M, Sakano S, Hill D, Strutt B, Thyssen S, Gray DA, Bhatia M (2003) Bone marrow-derived stem cells initiate pancreatic regeneration. Nat Biotechnol 21:763–770
23. Timper K, Seboek D, Eberhardt M, Linscheid P, Christ-Crain M, Keller U, Muller B, Zulewski H (2006) Human adipose tissue-derived mesenchymal stem cells differentiate into insulin, somatostatin, and glucagon expressing cells. Biochem Biophys Res Commun 341:1135–1140
24. Yamashita H (1997) Molecular pathogenesis of diabetic retinopathy. Nippon Rinsho 55(Suppl):960–965
25. Bringmann A, Pannicke T, Grosche J, Francke M, Wiedemann P, Skatchkov SN, Osborne NN, Reichenbach A (2006) Muller cells in the healthy and diseased retina. Prog Retin Eye Res 25:397–424
26. Arnhold S, Klein H, Klinz FJ, Absenger Y, Schmidt A, Schinkothe T, Brixius K, Kozlowski J, Desai B, Bloch W, Addicks K (2006) Human bone marrow stroma cells display certain neural characteristics and integrate in the subventricular compartment after injection into the liquor system. Eur J Cell Biol 85:551–565
27. Mori K, Gehlbach P, Ando A, McVey D, Wei L, Campochiaro PA (2002) Regression of ocular neovascularization in response to increased expression of pigment epithelium-derived factor. Invest Ophthalmol Vis Sci 43:2428–2434